ACS APPLIED MATERIALS & INTERFACES

Research Article

www.acsami.org

Measurement and Analysis of Adhesion Property of Lithium-Ion Battery Electrodes with SAICAS

Bongki Son,[†,§] Myung-Hyun Ryou,[†,§] Jaecheol Choi,[†] Taejoo Lee,[†] Hyung Kyun Yu,[‡] Jong Hun Kim,*[,‡] and Yong Min Lee*[,†]

[†]Department of Chemical and Biological Engineering, Hanbat National University, Deokmyoung-dong, Yuseong-gu, Daejeon 305-719, Republic of Korea

[‡]Battery R&D, LG Chem Ltd., 104-1 Moonji-dong, Yuseong-gu, Daejeon, 305-380, Republic of Korea

ABSTRACT: The adhesion strength of lithium-ion battery (LIB) electrodes consisting of active material, a nanosized electric conductor, and a polymeric binder is measured with a new analysis tool, called the Surface and Interfacial Cutting Analysis System (SAICAS). Compared to the conventional peel test with the same electrode, SAICAS gives higher adhesion strength owing to its elaborate cutting-based measurement system. In addition, the effects on the adhesion property of the polymeric binder type and content, electrode density, and measuring point are also investigated to determine whether SAICAS provides reliable results. The findings confirm SAICAS as an effective and promising tool to measure and analyze the adhesion properties of LIB electrodes.

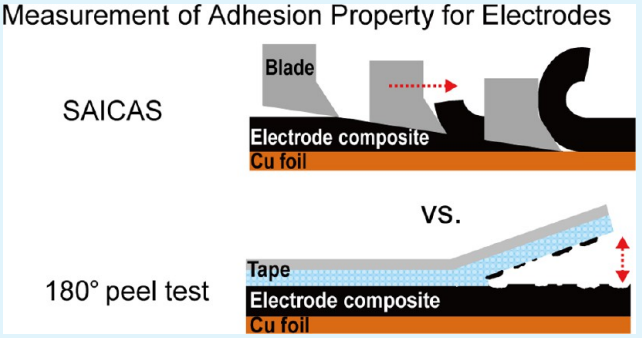

KEYWORDS: *adhesion property, peel test, electrode, surface and interfacial cutting analysis system (SAICAS), lithium-ion batteries*

INTRODUCTION

The application of lithium-ion batteries (LIBs) has been extended from small, mobile information technology (IT) devices to large-scale transportation or energy storage systems (ESSs) requiring much longer service time and higher reliability.[1−3] Therefore, in addition to two major components, electrode and electrolyte materials, other components such as the polymeric binder and current collector are also carefully selected to ensure LIBs against rapid decay in performance under severe operating and storage conditions. As recently reported, cell performance of silicon-based anodes was remarkably improved by simply substituting the commercial polymeric binder, polyvinylidene fluoride (PVdF), without further treatment for the active material.[4−6] In particular, good adhesion properties within the electrode composite and at its interface with the current collector should be well maintained to deliver the designed energy and power throughout the service period. However, there is no well-defined tool to analyze interfacial adhesion strength except for the conventional peel test,[4,7,8] which uses commercial adhesive tape (3 M Company) and a universal testing machine. Although the test indicates peel strength (kN/m), the results are also strongly dependent on measurement conditions, such as the type of adhesive tape, initial adhesion status between tape and sample surface, the mechanical sensitivity of the universal testing machine, etc. In addition, the adhesion strength indicated by the peel test is mainly derived from the surface adhesion property rather than the bulk material or the interface between electrode composite and current collector. In other words, we cannot obtain specific adhesion strength at a certain location, such as an interface between electrode composite and current collector or the internal cohesion at a point within the electrode composite.

In order to overcome these limitations, we try to reliably measure the adhesion strength of LIB electrodes via the Surface and Interfacial Cutting and Analysis System (SAICAS). The SAICAS system has been continuously developed by Daipla Wintes Co., Ltd. in Japan since 1990 and measures the adhesion strength or energy of a coating layer upon various substrates.[9−15] It uses a V-shaped microblade to cut the film while simultaneously measuring both horizontal and vertical forces (as shown in Figures 1 and 2), thereby reliably measuring adhesion strength at a specific depth. Surprisingly, this tool has not previously been used to investigate the adhesion property of cathodes and anodes for LIBs. Only a few groups have reported the adhesion property of LIB electrodes with different polymeric binder distributions.[16]

In this work, we newly applied the SAICAS tool to measure the adhesion strength of LIB anodes containing graphite active materials, a polymeric binder, and an electric conductor. First, anodes were prepared with different polymeric binder contents (2, 4, 8 wt %) and analyzed simultaneously by both SAICAS and the conventional peel test. In addition, the effects on adhesion strength of electrode density (1.4, 1.6, 1.8 g/cm^3),

Received: October 18, 2013
Accepted: December 9, 2013
Published: December 9, 2013

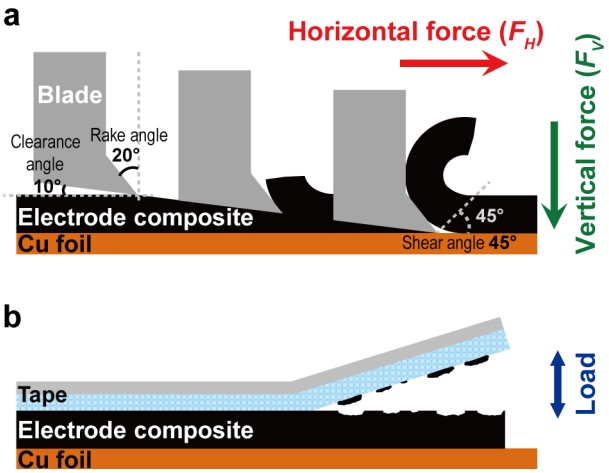

Figure 1. Schematic diagrams of measurement by (a) surface and interfacial cutting analysis system (SAICAS) and (b) conventional peel test.

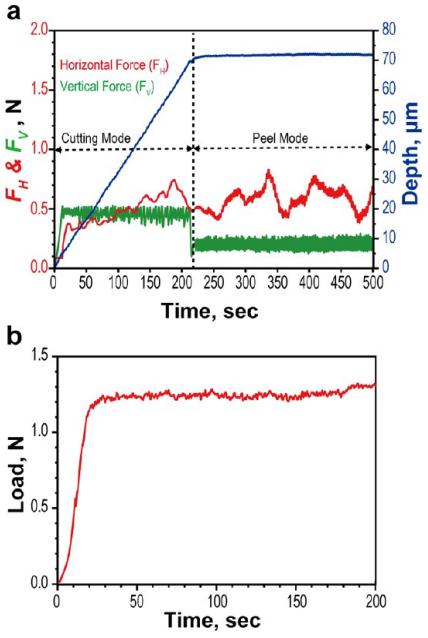

Figure 2. Representative data profiles measured by (a) SAICAS and (b) conventional peel test.

polymeric binder type (styrene–butadiene rubber/carboxymethyl cellulose vs polyvinylidene fluoride), and measuring point were also investigated to demonstrate the validity of the SAICAS method.

EXPERIMENTAL SECTION

Anode Preparation. A mixture of anode slurry containing natural graphite (MPG, Mitsubishi Chemical, Japan), an electric conductor (Super-P, Timcal, Switzerland), and a styrene–butadiene rubber (SBR, BM-400B, Zeon, Japan)/carboxymethyl cellulose (CMC, WS-C, Dahchi Kogyo Seiyaku, Japan) binder mixture in deionized water was prepared and cast onto Cu current collector foil (20 μm, Iljin Materials, Korea) using a doctor blade. The cast slurry was dried in the air at 60 °C for 2 h and then roll-pressed with a gap-control-type roll pressing machine (CLP-2025, CIS, Korea) to achieve the target density and thickness.

In order to conduct our research systemically, in this study, we categorized the types of anodes into three groups.

For the first group, the anode composition varied as shown in Table 1. The binder amount was increased from 2 to 8 wt % by decreasing

Table 1. Composition and Physical Properties of Anodes with Different Binder Contents

	unit	anode
active material (AM)	-	natural graphite
composition (AM/electric conductor/binder[a])	wt %	97:1:2 (1:1) 95:1:4 (2:2) 91:1:8 (4:4)
coating thickness	μm	50
loading level	mg/cm^2	7.0–8.0
electrode density	g/cm^3	1.6

[a]Binder: SBR 40 wt % solution, CMC 2 wt % solution.

the active material content while maintaining the electric conductor content at 1 wt %. However, the thickness and density of the electrode were maintained at 50 μm and 1.6 g/cm^3 (8 mg/cm^2), respectively, to ensure a similar internal structure.

For the second group, to investigate the effect of electrode density on adhesion property, the anodes with different densities (density: 1.4, 1.6, and 1.8 g/cm^3; loading level: 9.8, 11.2, and 12.6 mg/cm^2, respectively) were fabricated as keeping the same thickness (70 μm) and composition (95 wt % natural graphite, 1 wt % electric conductor, 4 wt % binder mixture).

Finally, to compare adhesion properties regarding the types of polymeric binder material, the anodes with polyvinylidene fluoride (PVdF, KF-1300, Kureha, Japan) binder were prepared using the *N*-methyl-2-pyrrolidone-based slurry (NMP, Sigma-Aldrich, USA). The anodes possess the same composition as those employing CMC binder (95 wt % natural graphite, 1 wt % electric conductor, and 4 wt % binder). Both anodes were also roll-pressed to have the same thickness of 50 μm and a density of 1.6 g/cm^3 (8 mg/cm^2).

Peel Test. A 12-mm-wide and 30-mm-long anode with varying binder content was attached to 3 M adhesive tape, and the peel strength of the anode sample was measured with a high-precision micromechanical test system (Delaminator Adhesion Test System; DTS Company, Menlo Park, CA, USA). The adhesive tape was removed by peeling at an angle of 180° at a constant displacement rate of 100 μm/s; the applied load was continuously measured, and force/displacement plots were produced.[4] Before and after testing, the surface morphologies of the anode and tape were observed by optical microscope (VHX-2000K, Keyence, Korea).

SAICAS Measurement. The adhesion strength at the interface between anode composite and current collector and at the middle point of the anode composite was measured via SAICAS. For this measurement, a boron nitride blade (width: 1 mm) having a shear angle of 45°, rake angle of 20°, and clearance angle of 10° was used (Figure 1a). During the test, the blade moves horizontally at 0.05 μm/s. In cutting mode, the blade also moves vertically with a force of 0.5 N until it reaches the Cu current collector; subsequently, in the peel mode, the vertical force is reduced from 0.5 N to 0.2 N to prevent further vertical movement. The adhesion strength can be calculated by averaging the horizontal forces during the peel mode, divided by the blade width. In addition, at least three measurements were conducted with each sample in order to obtain more reliable results. To help clear understanding, we provided the background trendlines featured in MS Excel 2010.

Morphological Analysis of Anodes. The surface- and cross-sectional morphology of anodes with different densities was characterized by field emission scanning electron microscope (FE-SEM, S4800, Hitachi, Japan). In order to prepare a cross-sectional specimen of each anode, it was cut by an argon-ion beam polisher (E3500, Hitachi) at a constant power of 2.1 W (6 kV and 0.35 mA) under a vacuum (<2.0 × 10^{-4} Pa).

dx.doi.org/10.1021/am404580f | ACS Appl. Mater. Interfaces 2014, 6, 526–531

RESULTS AND DISCUSSION

The schematic in Figure 1a shows the measurement of adhesion property via SAICAS. Since the system uses a slanted boron nitride blade, two perpendicular forces (horizontal and vertical) along the surface can be obtained simultaneously. In addition, two operating modes (peel mode at a constant horizontal rate; cutting mode with a constant vertical static load) are combined during successive passes of the blade in order to gradually cut to specific depth and measure horizontal force at that point. Therefore, the adhesion strength (P) of electrodes can be calculated by measuring the horizontal force ($F_{H,Peeling}$) during peeling at a constant rate, then dividing the averaged horizontal force by the width of the blade (w), as shown in eq 1:[9,14]

$$P = F_{H,Peeling}/w \text{ (kN/m)} \quad (1)$$

In addition, the shear stress (τ), which reflects the adhesion/cohesion strength within the electrode composite (measured in pressure-based values as MPa), can be calculated from horizontal force ($F_{H,Cutting}$) during the cutting mode, the width of the blade (w), electrode composite thickness (d), and shear angle (φ) via eq 2:[9,14]

$$\tau = F_{H,Cutting}/(2w \cdot d \cdot \cot \varphi) \text{ (MPa)} \quad (2)$$

The conventional peel test is also described in Figure 1b. Compared to the SAICAS, the conventional method can only measure adhesive strength between the surfaces of the electrode composite and the adhesive tape. As a result, it is not suited to evaluating adhesion strength at a specific depth within the electrode, e.g., at the interface between electrode composite and current collector.

Figure 2a and b present representative force profiles from the SAICAS and peel test, respectively. Contrary to the peel test profile, which shows only steady-state load (force), the SAICAS gives not only horizontal and vertical forces but also depth profiling. With an anode of 70 μm thickness and 1.6 g/cm^3 density, the depth increased linearly at a constant rate of 0.33 μm/s, because the vertical force was maintained at around 0.5 N during the cutting mode. When the cutting depth reached the anode composite thickness of 70 μm, the vertical force was reduced to 0.2 N, and the peel mode started to measure the horizontal force for adhesion strength at the interface. The horizontal force fluctuated greatly over time, which was due to intermittent detachment behavior of the anode composite from the current collector. Specifically, the horizontal force increases when the anode composite adheres to the current collector and then decreases following detachment.

The adhesion strengths of three anodes with different binder contents (see Table 1) were compared via SAICAS and the peel test. Figure 3 shows the load profiles with time in the peel test; the inset panel summarizes the corresponding adhesion strengths, which were calculated by dividing the average load value by the width (12 mm) of the 3 M tape. As expected, the adhesion strength increases (from 0.066 to 0.095 to 0.104 kN/m) with increasing binder content; however, adhesion strength plateaued at around 8 wt % binder content. Morphological changes to the anode and tape surfaces before and after the peel test are depicted via optical microscopic images presented in Figure 4. As the binder content increases, there is a significant reduction in the amount of active materials and electric conductors detached from the anode. From these adhesion strength data and optical microscopic images, 4 wt % SBR/CMC binder content can be regarded as the optimum composition for LIB anodes in this work.

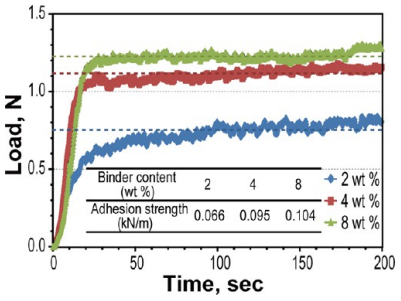

Figure 3. Load profiles of three anodes with different binder contents (2, 4, and 8 wt %) during the peel test (each adhesion strength is summarized within the inset).

The adhesion strength of the same anode group was also evaluated with SAICAS, and horizontal force and depth thickness profiles are presented in Figure 5. Similarly to the peel test, the adhesion strength between anode composite and current collector also increased from 0.282 to 0.408 to 0.479 kN/m with increased binder content. However, each adhesion strength value is approximately four times higher than the peel test summarized in Figure 3, because the SAICAS measures the horizontal force required to completely peel off the anode composite, as confirmed by the post-test images of the samples (See Figure 6). As a result, the peel test cannot give intrinsic adhesion strength, but only relative trends depending on tape type, initial adhesion strength between anode and tape, etc.

Another advantage of SAICAS is that shear stress (specific adhesion strength divided by cross-sectional area) during the cutting mode can also be obtained via eq 2. As summarized in Table 2, anodes with higher binder content can withstand increased shear stress. For example, the shear stress of the anode containing 8 wt % binder is 0.040 MPa, which is ~177% and ~110% higher than the anodes with 2 and 4 wt % binder contents, respectively. Considering this powerful capability to analyze the adhesion properties of LIB electrodes, various case studies have been conducted in this work.

In order to compare adhesion properties at different depths, SAICAS measurements with one anode of 70 μm thickness and 1.6 g/cm^3 density were repeated in the center of the anode composite and at the interface between anode composite and current collector. As shown in Figure 7, the adhesion strength (0.388 kN/m) and shear stress (0.042 MPa) within the center of the anode composite are slightly less than those at the interface (0.510 kN/m and 0.031 MPa), which implies that adhesion strength at the interface exceeds cohesion strength within the anode composite itself. Therefore, the horizontal force at the interface also shows greater fluctuation than that within the anode composite. As summarized in Table 3, the cohesion strengths within the center of the anode composite are around 75% of interfacial adhesion strengths regardless of anode densities. However, since the adhesion strength within the anode composite is much higher than that obtained from the conventional peel test (see Figure 3), SAICAS can give the intrinsic adhesion strength at a specific point.

Figure 8 shows the horizontal force and depth profiles of anodes with different densities (1.4, 1.6, and 1.8 g/cm^3, 70 μm thickness; and the same composition: 95 wt % active material, 1 wt % electric conductor, 4 wt % SBR/CMC binder). As the density increased, the adhesion strength at the interface

dx.doi.org/10.1021/am404580f | ACS Appl. Mater. Interfaces 2014, 6, 526−531

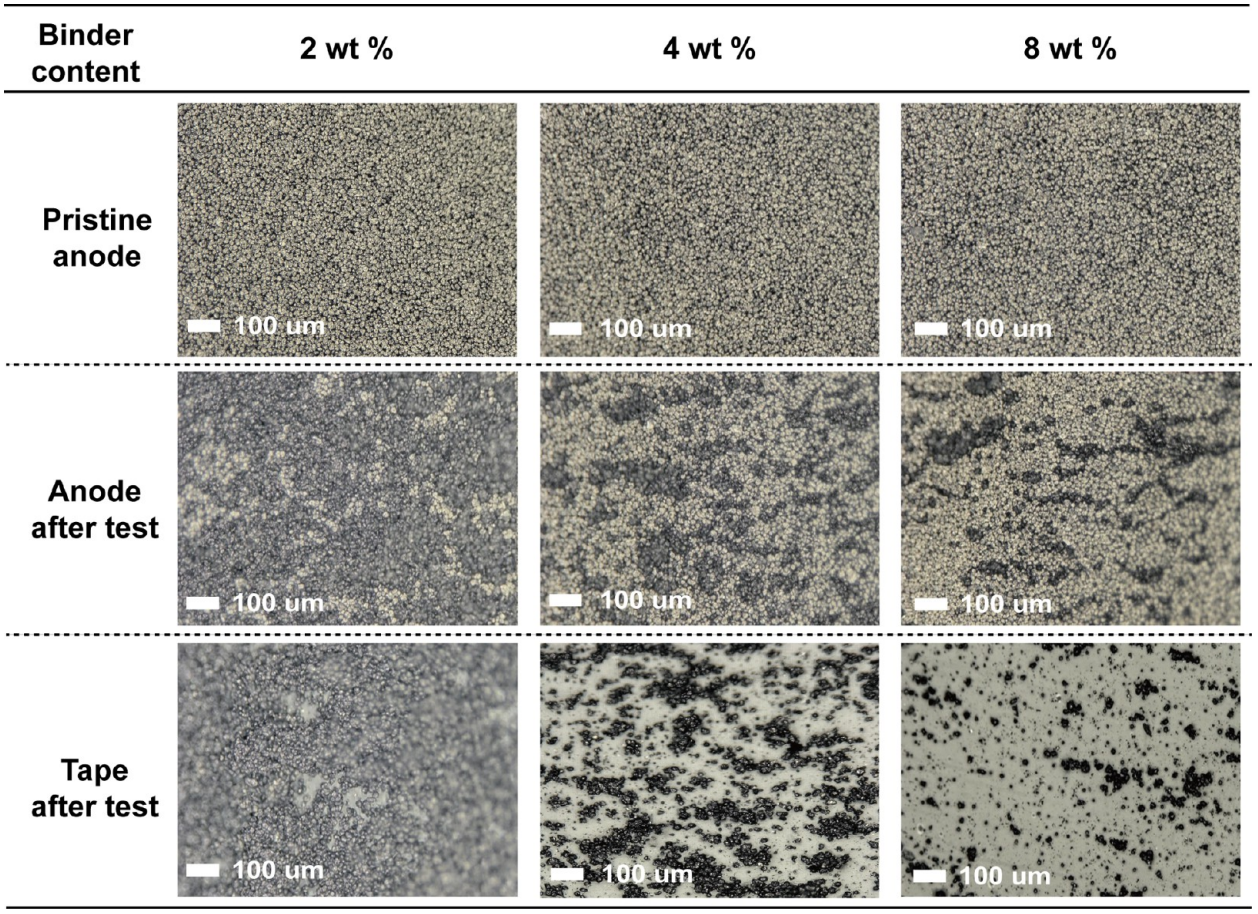

Figure 4. Optical microscopic images of pristine anodes with different binder contents (2, 4, and 8 wt %), and corresponding anodes and tapes after the peel test.

Table 2. Adhesion Strength and Shear Stress of Anodes with Different Binder Contents

binder content (wt %)	2	4	8
adhesion strength (kN/m)	0.282	0.408	0.479
shear stress (MPa)	0.022	0.036	0.040

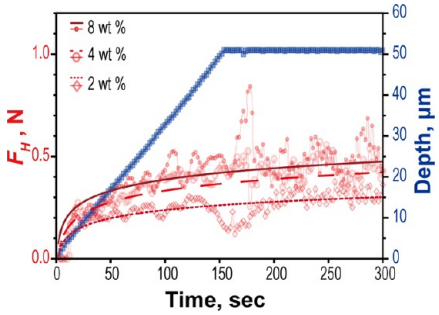

Figure 5. Force and depth profiles of three anodes with different binder contents (2, 4, and 8 wt %) measured by SAICAS.

between anode composite and current collector also increased from 0.408 kN/m to 0.552 kN/m, which is an improvement of approximately 35%. In order to investigate the effect of changing anode morphology on adhesion property, the surface and cross-sectional SEM images of anodes are also presented in Figure 9. Considering that the true density of natural graphite is about 2.1, the density of 1.8 g/cm^3 can be considered as the

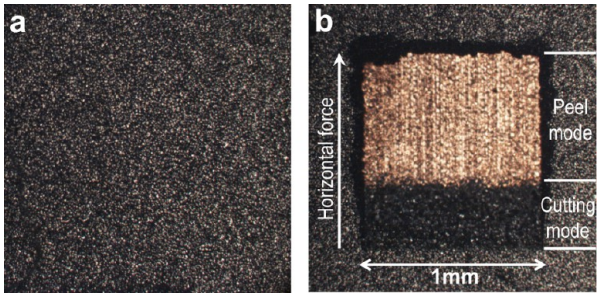

Figure 6. Optical microscopic images of anodes (a) before and (b) after SAICAS measurement.

Table 3. Adhesion Strength of Anodes with Different Electrode Densities at 70 μm (Anode Composite/Current Collector Interface) and 40 μm Depths

density (g/cm^3)		1.4	1.6	1.8
adhesion strength (kN/m)	① 70 μm depth (interface)	0.408	0.510	0.552
	② 40 μm depth	0.314	0.388	0.412
	ratio of ② to ①	0.77	0.76	0.75

maximum for commercially available graphite-based anodes. From the corresponding images and porosimeter measurements, the anode porosity is greatly decreased from 35.5% to 17.5%, producing more contact points between anode constituents (active materials, electric conductor and binders)

dx.doi.org/10.1021/am404580f | ACS Appl. Mater. Interfaces 2014, 6, 526−531

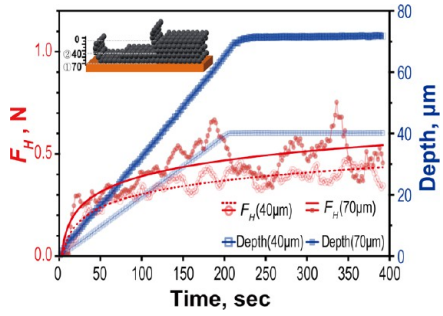

Figure 7. Force and depth profiles of an anode at 70 μm (anode composite/current collector interface) and 40 μm depths measured by SAICAS.

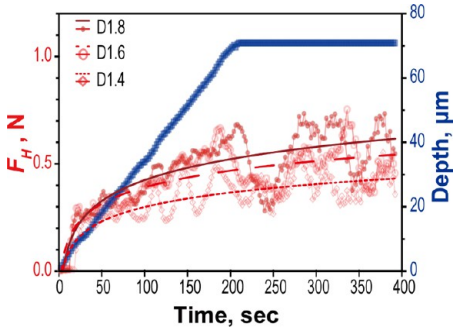

Figure 8. Force and depth profiles of three anodes with different electrode densities (1.4, 1.6, and 1.8 g/cm^3) measured by SAICAS.

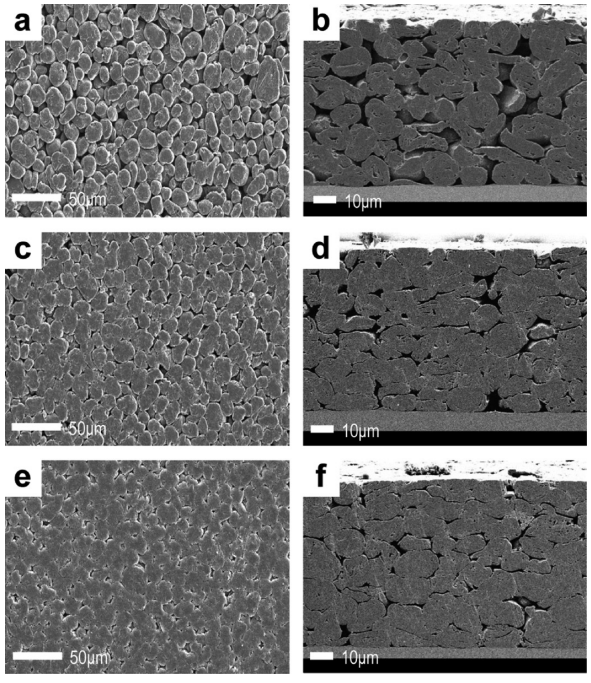

Figure 9. Surface and cross-sectional SEM images of three anodes with different electrode densities (a, b) 1.4 g/cm^3, (c, d) 1.6 g/cm^3, and (e, f) 1.8 g/cm^3, respectively.

and at the interface between anode composite and current collector. Therefore, this enhancement of adhesion strength could be ascribed to the greater number of contact points achieved with higher anode density.

Finally, the effect of binder type on adhesion property is also evaluated with an aqueous-based SBR/CMC binder and nonaqueous-based PVdF binder, and the force and depth profiles are shown in Figure 10. Although the same binder

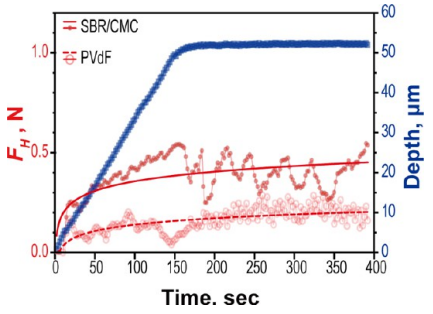

Figure 10. SAICAS force and depth profiles for two anodes prepared with the SBR/CMC and PVdF binder systems, respectively.

content of 4 wt % was introduced into both anodes, the adhesion strength of the anode with PVdF binder was 0.228 kN/m, which is ~55% of that with SBR/CMC. The aqueous SBR/CMC binder system therefore achieves greater adhesion and is more attractive for designs utilizing higher energy density. Also, contrary to the large fluctuations in horizontal force observed with the SBR/CMC binder system, the anode with PVdF binder shows very narrow fluctuation, which may be related to the weaker, so-called fiber-like adhesion mechanism of PVdF. As reported in many previous studies,[17−19] the SBR/CMC binder provides a strong point-contact adhesion due to SBR rubber particles on the scale of tens of nanometers. Therefore, SAICAS can also provide useful information on adhesion mechanisms.

CONCLUSIONS

The SAICAS can determine more localized adhesion properties of LIB anodes compared to the conventional peel test, because it measures adhesion forces while completely peeling off the anode composite. For the same anode design, the adhesion strength indicated by SAICAS was at least four times greater than that from the peel test. Also, the effects on adhesion strength of binder content, electrode density, and depth thickness were also well verified with SAICAS. In particular, some information on the adhesion mechanism could be derived from fluctuations in force patterns. The findings suggest SAICAS as a very promising tool for analysis of LIB electrodes in the near future.

AUTHOR INFORMATION

Corresponding Authors

*Tel.: +82-42-821-1549. Fax: +82-42-821-1692. E-mail: yongmin.lee@hanbat.ac.kr.

*Tel.: +82-42-866-2957. Fax: +82-42-862-1981. E-mail: johnkim@lgchem.com.

Author Contributions

[§]These authors contributed equally to this work.

Notes

The authors declare no competing financial interest.

ACKNOWLEDGMENTS

This research was financially supported by Chungcheong Leading Industry Promotion Project of the Korean Ministry of Trade, Industry and Energy and the National Research Foundation of Korea (NRF) through the Human Resource

Training Project for Regional Innovation. We also thank Sungmoon Systech Corp. in Korea for helping us use the SAICAS instrument for this work.

REFERENCES

(1) Wang, X.; Sone, Y.; Naito, H.; Yamada, C.; Segami, G.; Kibe, K. *J. Power Soures* **2006**, *161*, 594−600.
(2) Ryou, M.-H.; Lee, D. J.; Lee, J.-N.; Lee, Y. M.; Park, J.-K.; Choi, J. W. *Adv. Energy Mater.* **2012**, *2*, 645−650.
(3) Zackrisson, M.; Avellán, L.; Orlenius, J. *J. Clean. Prod.* **2010**, *18*, 1519−1529.
(4) Ryou, M.-H.; Kim, J.; Lee, I.; Kim, S.; Jeong, Y. K.; Hong, S.; Ryu, J. H.; Kim, T.-S.; Park, J.-K.; Lee, H.; Choi, J. W. *Adv. Mater.* **2013**, *25*, 1571−1576.
(5) Kovalenko, I.; Zdyrko, B.; Magasinski, A.; Hertzberg, B.; Milicev, Z.; Burtovyy, R.; Luzinov, I.; Yushin, G. *Science* **2011**, *334*, 75−79.
(6) Koo, B.; Kim, H.; Cho, Y.; Lee, K. Y.; Choi, N.-S.; Cho, J. *Angew. Chem., Int. Ed.* **2012**, *51*, 1−7.
(7) Chen, L.; Xie, X.; Xie, J.; Wang, K.; Yang, J. *J. Appl. Electrochem.* **2006**, *36*, 1099−1104.
(8) Park, H.-K.; Kong, B.-S.; Oh, E.-S. *Electrochem. Commun.* **2011**, *13*, 1051−1053.
(9) Nagai, N.; Imai, T.; Terada, K.; Seki, H.; Okumura, H.; Fujino, H.; Yamamoto, T.; Nishiyama, I.; Hatta, A. *Surf. Interface Anal.* **2002**, *34*, 545−551.
(10) Horibe, H.; Fujita, M.; Nishiyama, I.; Yoshikado, A. *Jpn. J. Appl. Phys.* **2005**, *44*, 8673−8675.
(11) Saito, F.; Fujii, Y.; Nagashima, Y.; Yotoriyama, T.; Nakao, A.; Suzuki, Y.; Iwaki, M.; Nishiyama, I.; Hyodo, T. *Phys. Status Solidi C* **2007**, *4*, 3718−3721.
(12) Saito, F.; Nishiyama, I.; Hyodo, T. *Mater. Lett.* **2009**, *63*, 2257−2259.
(13) Oyane, A.; Yokoyama, Y.; Kasahara, M.; Ichinose, N.; Saito, M.; Ito, A. *Mater. Sci. Eng., C* **2009**, *29*, 1681−1686.
(14) Saito, F.; Nishiyama, I.; Hyodo, T. *Surf. Coat. Technol.* **2010**, *205*, 419−422.
(15) Iwamori, S.; Hasegawa, N.; Uemura, A.; Tanabe, T.; Nishiyama, I. *Vacuum* **2010**, *84*, 592−595.
(16) Fukumitsu, H.; Omori, M.; Morooka, K.; Terada, K.; Shibahara, K.; Takahashi, T.; Shimada, S.-I.; Suehiro, S.; Ohashi, K. Depth profile of binder and its influence on property of electrode and battery. In *Proceeding of the 53rd Battery Symposium in Japan*, Fukuoka, Japan, 2012; Electrochemical Society of Japan: Tokyo, 2012.
(17) Buqa, H.; Holzapfel, M.; Krumeich, F.; Veit, C.; Novák, P. *J. Power Soures* **2006**, *161*, 617−622.
(18) Lee, J.-H.; Paik, U.; Hackley, V. A.; Choi, Y.-M. *J. Electrochem. Soc.* **2005**, *152*, A1763−A1769.
(19) Yen, J.-P.; Chang, C.-C.; Lin, Y.-R.; Shen, S.-T.; Hong, J.-L. *J. Electrochem. Soc.* **2013**, *160*, A1811−A1818.